

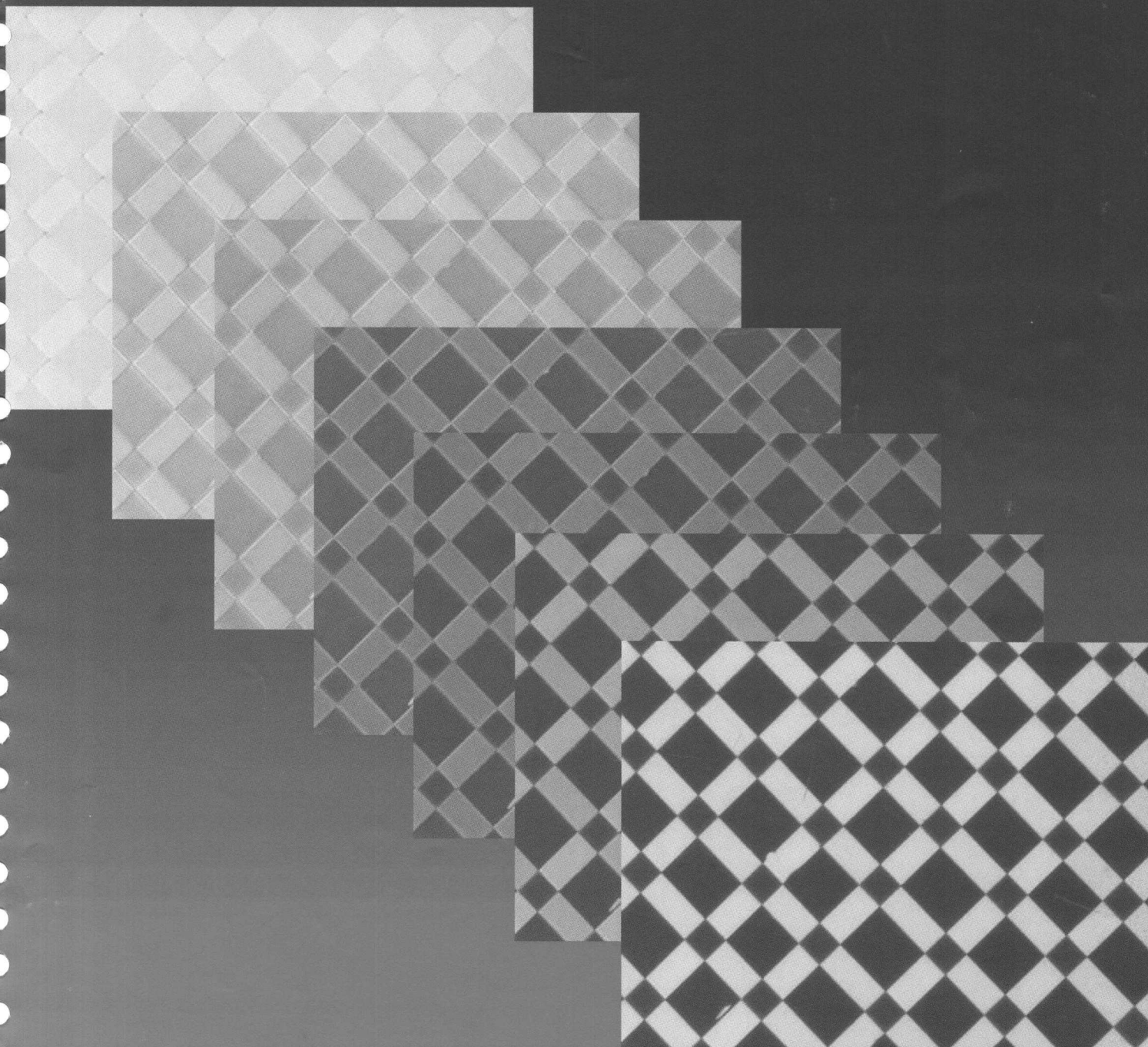
D10488

ADVMEW  
ISSN 0935-9648  
Vol. 16, No. 18  
September 16, 2004



WILEY-  
VCH

# ADVANCED MATERIALS



Alignment of Liquid Crystals by Microrubbing

- [1] a) O. Kahn, *Molecular Magnetism*, VCH, New York 1993. b) O. Kahn, *Adv. Inorg. Chem.* **1995**, 43, 179.
- [2] a) A. Caneschi, D. Gatteschi, R. Sessoli, P. Rey, *Acc. Chem. Res.* **1989**, 22, 392. b) A. Caneschi, D. Gatteschi, P. Rey, *Prog. Inorg. Chem.* **1991**, 39, 331.
- [3] a) A. Caneschi, D. Gatteschi, N. Lalio, C. Sangregorio, R. Sessoli, G. Venturi, A. Vindigni, A. Rettori, M. G. Pini, M. Novak, *Angew. Chem. Int. Ed.* **2001**, 40, 1760. b) A. Caneschi, D. Gatteschi, N. Lalio, C. Sangregorio, R. Sessoli, G. Venturi, A. Vindigni, A. Rettori, M. G. Pini, M. Novak, *Europhys. Lett.* **2001**, 58, 771.
- [4] R. J. Glauber, *J. Math. Phys.* **1963**, 4, 294.
- [5] a) R. Clérac, H. Miyasaka, M. Yamashita, C. Coulon, *J. Am. Chem. Soc.* **2002**, 124, 12837. b) H. Miyasaka, R. Clérac, K. Mizushima, K. Sugiura, M. Yamashita, W. Wernsdorfer, C. Coulon, *Inorg. Chem.* **2003**, 42, 8203.
- [6] a) R. Lescouëzec, J. Vaissermann, C. Ruiz-Pérez, F. Lloret, R. Carasco, M. Julve, M. Verdager, Y. Dromzée, D. Gatteschi, W. Wernsdorfer, *Angew. Chem. Int. Ed.* **2003**, 42, 1483. b) L. M. Toma, R. Lescouëzec, F. Lloret, M. Julve, J. Vaissermann, M. Verdager, *Chem. Commun.* **2003**, 1850.
- [7] T. F. Liu, D. Fu, S. Gao, Y. Z. Zhang, H. L. Sun, G. Su, Y. J. Liu, *J. Am. Chem. Soc.* **2003**, 125, 13976.
- [8] Crystal data for **1**:  $C_{22}H_{34}CoCuN_2O_{12}$ ,  $M_r = 640.98$ , monoclinic, space group  $C2/m$ ,  $a = 15.930(3)$ ,  $b = 8.702(3)$ ,  $c = 10.602(3)$  Å,  $\beta = 99.54(2)^\circ$ ,  $V = 1449.4(7)$  Å<sup>3</sup>,  $T = 293$  K,  $Z = 2$ ,  $\rho_{\text{calcd}} = 1.453$  g cm<sup>-3</sup>,  $\mu(\text{Mo K}\alpha) = 1.365$  mm<sup>-1</sup>. 2212 unique reflections, and 1446 observed with  $I > 2\sigma(I)$ . All the measured independent reflections were used in the analysis. The structure was solved by direct methods and refined with full-matrix least-squares technique on  $F^2$  using the SHELXS-97 and SHELXL-97 programs. The hydrogen atoms from the organic ligand were calculated and refined with isotropic thermal parameters, while those from the water molecules were neither found nor calculated. Refinement of 110 variables with anisotropic thermal parameters for all non-hydrogen atoms gave  $R = 0.0531$  and  $R_w = 0.1107$ , with  $S = 1.004$ . The final Fourier-difference map showed maximum and minimum height peaks of 0.51 and  $-0.34$  e Å<sup>-3</sup>. Crystallographic data (excluding structure factors) for the structure reported in this paper have been deposited with the Cambridge Crystallographic Data Centre as supplementary publication no. CCDC-227520. Copies of the data can be obtained free of charge on application to CCDC, 12 Union Road, Cambridge CB21EZ, UK (fax: (+44) 1223-336-033; e-mail: deposit@ccdc.cam.ac.uk).
- [9] Variable-temperature (1.8–300 K) DC and AC magnetic susceptibility measurements and variable-field (0–5 T) DC magnetization measurements were carried out on a polycrystalline sample of **1** with a Quantum Design SQUID magnetometer. The magnetic data were corrected for the diamagnetism of the constituent atoms and the sample holder.
- [10] A. Gulbrandsen, J. Sletten, K. Nakatani, Y. Pei, O. Kahn, *Inorg. Chim. Acta* **1993**, 212, 271.
- [11] We have performed a preliminary analysis of the magnetic data of **1** through the branch chain model previously developed for the related oxamato-bridged bimetallic chain compound  $[\text{CoCu}(\text{pbaOH})(\text{H}_2\text{O})_3] \cdot 2\text{H}_2\text{O}$  [ $\text{pbaOH} = N,N'$ -2-hydroxy-1,3-propylenebis(oxamato)]; P. J. Van Kroningsbrugge, O. Kahn, K. Nakatani, Y. Pei, J. P. Renard, M. Drillon, P. Legoll, *Inorg. Chem.* **1990**, 29, 3325. In this model, it is assumed that only  $z$  components of spin and orbital momenta are coupled and that the applied magnetic field is along the quantization axis. The corresponding Hamiltonian is then written as  $H = \sum_i [-J[S_{\text{Co},i(z)}(S_{\text{Cu},i(z)} + S_{\text{Cu},i-1(z)})] + J' \cdot L_{\text{Co},i(z)} \cdot S_{\text{Co},i(z)} + D \cdot L_{\text{Co},i(z)}^2 - \beta \cdot H_z(g_{\text{Co}} \cdot S_{\text{Co},i(z)} + g_{\text{Cu}} \cdot S_{\text{Cu},i(z)} + k \cdot L_{\text{Co},i(z)})]$ , where  $i$  runs over CoCu units,  $L_{\text{Co}}$  is the orbital momentum,  $J$  and  $J'$  are the exchange and spin-orbit coupling parameters,  $\kappa$  and  $D$  are the orbital reduction and local anisotropy parameters of the cobalt(II) ion, and  $g_{\text{Co}}$  and  $g_{\text{Cu}}$  are the Landé factors. Least-squares fit of the  $\chi_M T$  data of **1** through this model in the temperature range 30–290 K reproduces well the observed minimum (solid line in the inset of Fig. 2a), with  $J = -26.6$  cm<sup>-1</sup>,  $J' = 91.5$  cm<sup>-1</sup>,  $\kappa = 0.8$ ,  $D = -188.0$  cm<sup>-1</sup>,  $g_{\text{Co}} = 2.38$ , and  $g_{\text{Cu}} = 2.05$ . The antiferromagnetic exchange coupling between copper(II) and cobalt(II) ions in **1** is somewhat stronger than that reported for  $[\text{CoCu}(\text{pbaOH})(\text{H}_2\text{O})_3] \cdot 2\text{H}_2\text{O}$  ( $J = -18.0$  cm<sup>-1</sup>). The fact that the copper atom in **1** lies in the oxamato plane ( $\text{CuN}_2\text{O}_2$  chromophore in a square-planar surrounding), whereas it is out of this mean plane in the related pbaOH compound ( $\text{CuN}_2\text{O}_3$  chromophore in a square-pyramidal environment), leads to a better overlap of the magnetic orbitals through the  $\sigma$ -in-plane exchange pathway, and thus to a larger antiferromagnetic coupling in **1**. The effective spin-orbit coupling can be related with the spin-orbit coupling parameter  $\lambda$  through the expression  $J' = -A\kappa\lambda$ . This gives  $\lambda = -110$  cm<sup>-1</sup> (with  $A = 3/2$ ) for the cobalt(II) ion in **1** (compared with  $\lambda_0 = -180$  cm<sup>-1</sup> for the free ion).
- [12] S. M. J. Aubin, Z. Sun, L. Pardi, J. Krzystek, K. Folding, L. C. Brunel, A. L. Rheingold, G. Christou, D. N. Hendrickson, *Inorg. Chem.* **1999**, 38, 5329.

## Patterned Alignment of Liquid Crystals by $\mu$ -Rubbing\*\*

By Soney Varghese, Sunil Narayanankutty, Cees W. M. Bastiaansen,\* Gregory P. Crawford, and Dirk J. Broer

Alignment layers are extensively used in the production of liquid crystal displays (LCDs) in order to orient the liquid crystal molecule to give a desired optical effect.<sup>[1–6]</sup> For instance, planar alignment of liquid crystals—long axes of molecules in the plane of the substrate—is often enforced with specific polyimide layers, in combination with mechanical rubbing (buffing) procedure, producing unidirectional alignment that can propagate over macroscopic distances. Polyimides are usually preferred because of their excellent properties with respect to chemical resistance, thermal stability, adhesion

[\*] Dr. C. W. M. Bastiaansen, S. Varghese, Prof. G. P. Crawford, Prof. D. J. Broer  
Department of Polymer Technology  
Faculty of Chemistry and Chemical Engineering  
Eindhoven University of Technology  
P.O. Box 513, NL-5600 MB Eindhoven (The Netherlands)  
E-mail: c.w.m.bastiaansen@tue.nl

Dr. S. Narayanankutty  
Department of Polymer Science and Rubber Technology  
Cochin University of Science and Technology  
Cochin-22 (India)

Prof. D. J. Broer  
Philips Research Laboratories, Prof. Holstlaan 4 (WB 72),  
5656 AA Eindhoven, The Netherlands  
E-mail: dick.broer@philips.com

[\*\*] The authors would like to acknowledge David Trimbach, Pit Teunissen and Peter Minten (GTD) at Eindhoven University of Technology for their support. Funding of this project was provided by Netherland University Federation for International Collaboration (Nuffic).

to substrates, high resistivity and transparency in the visible spectrum. The mechanical rubbing of polyimides is performed with a velvet-type synthetic cloth, which comes in direct contact with the polyimide. Recently there have been a variety of noncontact routes for patterning alignment layers in LCDs. The patterned alignment of cinnamates, coumarins, and special polyimide coated surfaces was extensively investigated using lithographic techniques in combination with linearly polarized light.<sup>[7-10]</sup> The direct writing with low-energy ion-beams on amorphous, inorganic thin films was also used as a suitable noncontact method for patterned alignment.<sup>[11]</sup> Patterned alignment of liquid crystals onto printed self-assembled monolayers was also explored by a number of groups.<sup>[12-14]</sup> At the moment, none of the above mentioned techniques can be used extensively in the production of LCDs which is predominantly related to the poor control of the surface pre-tilt angle, image retention phenomena, and/or to complex fabrication routes.

More recently, the micropatterning of alignment layers has been performed with an extremely sharp stylus by Rosenblatt and co-workers<sup>[15,16]</sup> and also Yokoyama and co-workers<sup>[17]</sup> has used the micropatterning of surfaces in order to create a tristable nematic liquid crystal device. The use of direct writing techniques with a sharp stylus imposes severe limitations on the production of alignment layers for large-area displays (i.e., the typical width of a single recorded line is less than 100 nm and consequently lengthy recording times are required in order to produce a single pixel or, more importantly, a large-area substrate). Therefore, a need persists for new methods to produce patterned, well-defined alignment layers, which are compatible with large scale production techniques. Here, we report on a simple and efficient tool which is

used for patterning alignment layers that is based on the rubbing of polyimides with a macroscopic, metallic object. The prime objective is to explore new routes for the micropatterning of alignment layers that may be more compatible with LCD production routes.

In an initial set of experiments, the alignment of liquid crystals on polyimide substrates after rubbing with a relatively large ( $d=1$  mm) metallic sphere was investigated. Of course despite the large diameter, the contact area is still of the order of tens of micrometers. The sphere was polished and has typically a surface roughness of  $\sim 8$  nm. The sphere is connected to a cantilever, which accurately controls the force (1–100 N) exerted on the polyimide coated substrate by the sphere (Fig. 1c). The substrate is mounted on a translational stage that moves with a pre-determined velocity ( $10$  mm  $\text{min}^{-1}$ ). The rubbing of a spin-coated, baked polyimide was initially investigated. In Figures 1a,b scanning probe microscopy (SPM) measurements are shown of the polyimide surfaces, which illustrate that the polyimide layers are extremely smooth outside the recorded patterns on the SPM scale. Within the recorded lines, irregular spaced grooves are observed (see the height profile in Fig. 1), which are oriented in the recording direction; some debris is also notable in Figure 1.

In Figure 2, the line width of the recorded patterns is plotted as a function of the applied load. Experimental data are used originating from line width measurements that are based on SPM (on bare substrates) and optical microscopy (on cells filled with liquid crystal). It is shown that a relationship exists between the applied load and the line width of the pattern. Moreover, this graph illustrates the flexibility that we have in creating different line widths using a metallic sphere of diameter 1 mm.

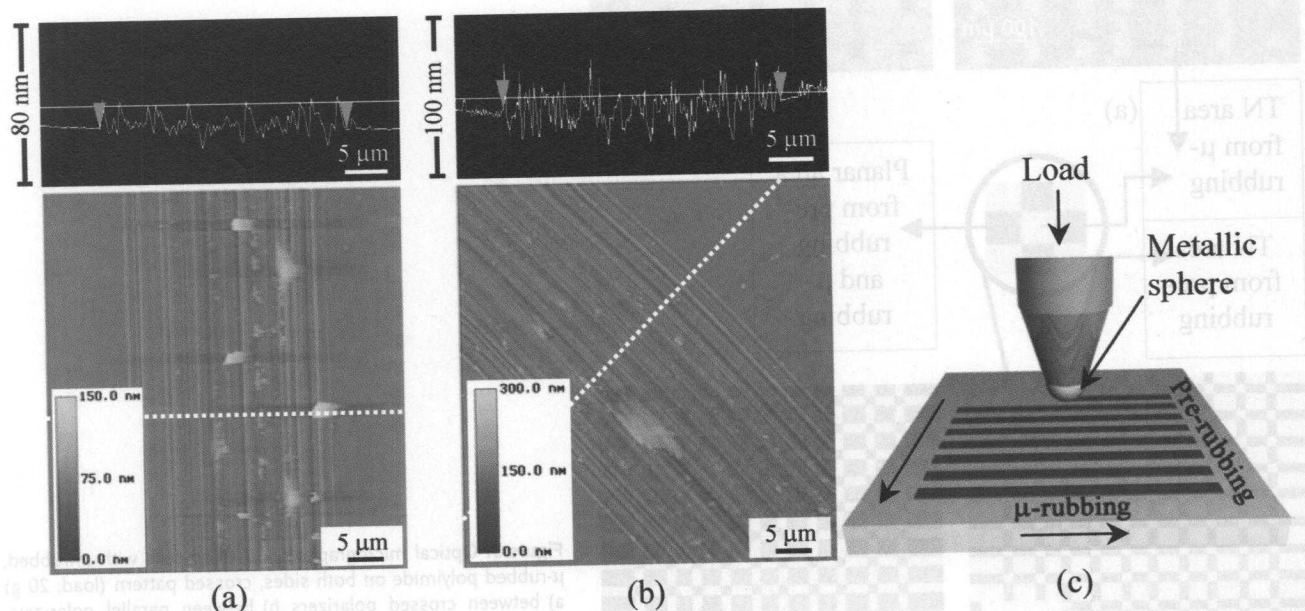


**Figure 1.** Scanning probe microscopy images of  $\mu$ -rubbed polyimides with a load of 20 g. a) Unrubbed,  $\mu$ -rubbed polyimide and its height profile drawn along the dotted line b)  $\mu$ -rubbed polyimide films which were pre-rubbed with a velvet cloth and c) a schematic of the metallic sphere used in the  $\mu$ -rubbing process.

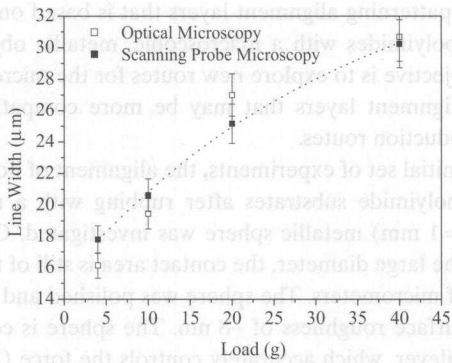


**Figure 2.** Variation of line width with applied load, measured with atomic force microscopy and with polarized optical microscopy (E7 filled cell).

Thin cells (18 μm) were constructed using two substrates with several parallel recorded μ-rubbed lines. The top and bottom substrate had μ-rubbed directions that were orthogonal. In Figures 3a,b typical optical micrographs are shown of cells filled with a liquid crystal (E7). Outside the μ-rubbed regions, the typical Schlieren texture of a non-aligned nematic liquid crystal is observed. Planar alignment of liquid crystals was observed in the areas with a μ-rubbed line pattern on one side and a non-rubbed polyimide layer on the other side.

Twisted nematic (TN) regions are observed between the crossed μ-rubbed lines, which illustrates that the μ-rubbing tends to induce a uniform planar alignment.

Next, a pre-rubbing procedure was performed with a velvet cloth (conventional rubbing), which induces a homogeneous planar alignment in the liquid crystal layer. The μ-rubbing of these polyimide layers followed in a direction perpendicular to the pre-rubbing direction. Figure 1b shows SPM images of the pre-rubbed, μ-rubbed substrates. Outside the recorded patterns, the subtle evidence of grooves from the first rubbing procedure can be observed. Upon μ-rubbing, well-defined line patterns are generated with irregular groove widths that are parallel to the μ-rubbing direction. The actual roughness originating from the μ-rubbing procedure exceeds the roughness from the conventional rubbing even at low loads (<2 g), which is the first indication that initial buffing is erased by the μ-rubbing. From the SPM experiments the depth of the μ-rubbed grooves was determined to be ~10–20 nm, which is almost one order of magnitude less than the thickness of the spin-coated polyimide film (~100 nm).

Cells were constructed with two homogeneously pre-rubbed polyimide layers that contained several μ-rubbed lines. In these cells, the rubbing directions are mutually orthogonal which creates several regions in the same cell: i) twisted nematic regions originating from the pre-rubbing procedure

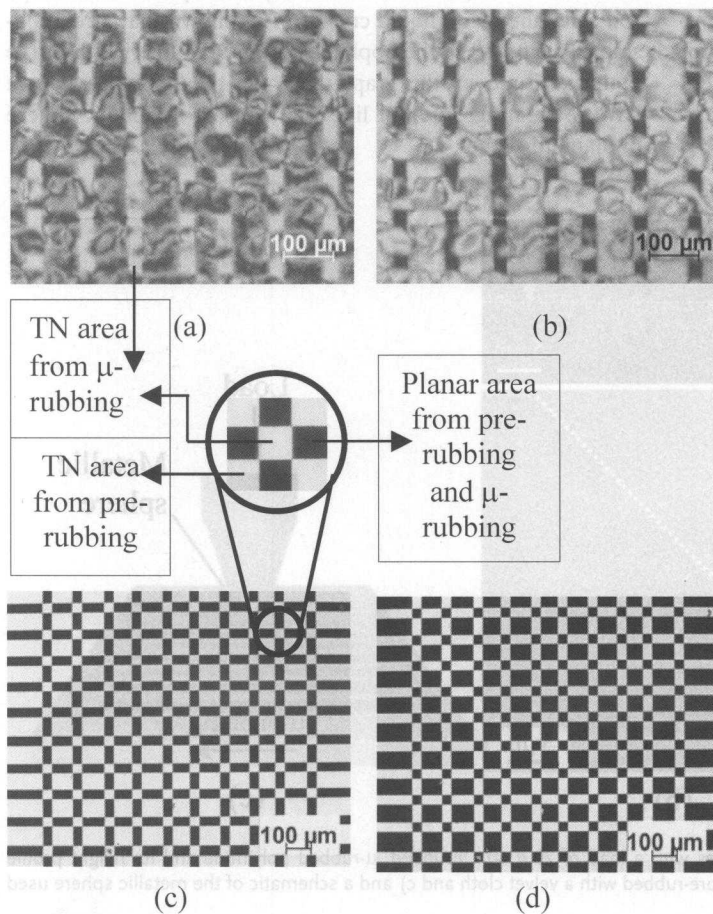


**Figure 3.** Optical micrographs of E7 filled cells with unrubbed, μ-rubbed polyimide on both sides, crossed pattern (load: 20 g) a) between crossed polarizers b) between parallel polarizers. c) Optical micrographs of LC cell with pre-rubbed polyimide substrate having μ-rubbed, crossed pattern on both sides are shown between crossed polarizers and d) between parallel polarizers.

with a velvet cloth; ii) planar regions originating from the combination of a homogeneous pre-rubbed layer with a  $\mu$ -rubbed line; and iii) twisted nematic regions originating from the  $\mu$ -rubbing procedure (Figs. 3c,d). The optical micrographs illustrate that well-defined regions with a different liquid crystal configuration are obtained.

In Figure 4, optical micrographs are shown of a LC cell during the application of an electrical field. The twisted nematic regions originating from the buffing and  $\mu$ -rubbing have similar threshold voltages. In other regions (originally planar) the threshold voltage is slightly lower than the TN regions as predicted by a Fredericks transition model.<sup>[18]</sup> Also, the disclination lines at the interfaces between the various alignment regions are clearly observable and become more pronounced at higher voltages.

In Figure 5a, the switching characteristics of a conventional rubbed TN cell are compared with the TN areas generated by  $\mu$ -rubbing process of pre-rubbed polyimide. The TN area created by the  $\mu$ -rubbing process shown in Figure 3 is too small ( $28 \mu\text{m}^2$ ) to perform an accurate electro-optical measurement. To overcome this problem we replaced the metallic ball with a well polished metallic ring with a width of  $500 \mu\text{m}$  having chamfered edges. The ring apparatus is attached to the translational stage under the appropriate load (see Fig. 5a, inset). By implementing this process we generated multiple pattern, analogues to the metallic sphere method (Fig. 1c) with larger line widths. We carefully aligned the edges of the rubbed regions so they would coincide with one another to achieve uniformity of the  $\mu$ -rubbing region over a large area. From the graph it is clear that the TN areas formed by the  $\mu$ -rubbing and the conventional rubbing process switch nearly at the

same voltage with only small noticeable difference. The transition slopes of the two curves presented in Figure 5a were nearly identical; however, the  $\mu$ -rubbed transmission curve approached a zero value more slowly at high voltages (i.e., lower contrast ratio). We attribute this to a distribution in the liquid crystal alignment along the preferred azimuthal direction (i.e.,  $\mu$ -rubbed direction). One possible source of this phenomenon is the nonuniformity of the polished ring. Figure 5b shows the dynamic response times (measured between 10 % and 90 % transmission) for the TN area generated from the pre-rubbing and  $\mu$ -rubbing process. As can be observed directly from Figure 5b, there is essentially no difference between the dynamic response times of the  $\mu$ -rubbed samples as compared to conventional rubbed samples, and the off-state (relaxation) is essentially constant and the on-state scales as the inverse voltage as expected from theory.<sup>[18]</sup>

Studies were extended in order to measure the electro-optic performance of homogeneously aligned samples. Anti-parallel  $\mu$ -rubbed cells were made with the above mentioned metallic ring with a cell thickness of  $18 \mu\text{m}$ . The cell was placed at  $45^\circ\text{C}$  between cross polarizers for the electro-optical measurement. The typical transmission voltage curve has been observed for the planar aligned sample, which oscillates due to the changes in birefringence induced by the voltage (Fig. 5c).<sup>[19]</sup> Again  $\mu$ -rubbed area has a similar but slightly higher switching voltage. This was the same phenomenon observed in the TN case presented in Figure 5a.

The slight increase in threshold voltage for the  $\mu$ -rubbed area compared to conventional rubbing can be attributed to an increase in anchoring energy (highly unlikely) or a decrease in surface pretilt angle. The pretilt of the  $\mu$ -rubbed and

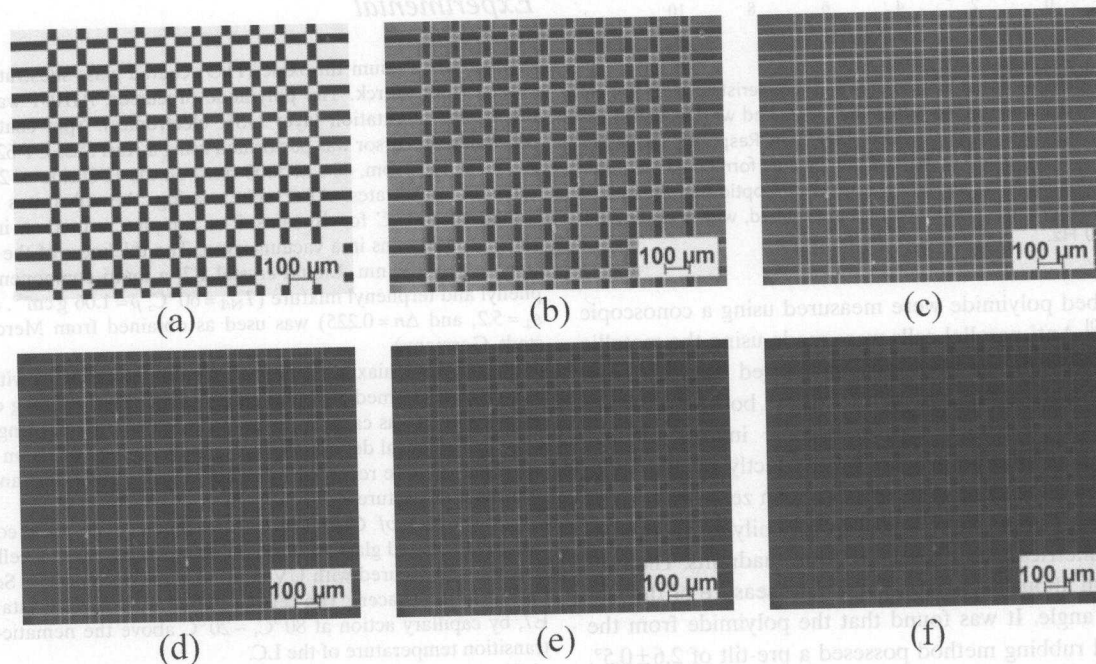


**Figure 4.** Optical micrographs of LC cell with pre-rubbed polyimide having  $\mu$ -rubbed patterns viewed between crossed polarizers, response under electric field. a)  $V=0$ , b)  $V=1.0$ , c)  $V=2.0$ , d)  $V=4.0$ , e)  $V=6.0$ , f)  $V=10.0$ .

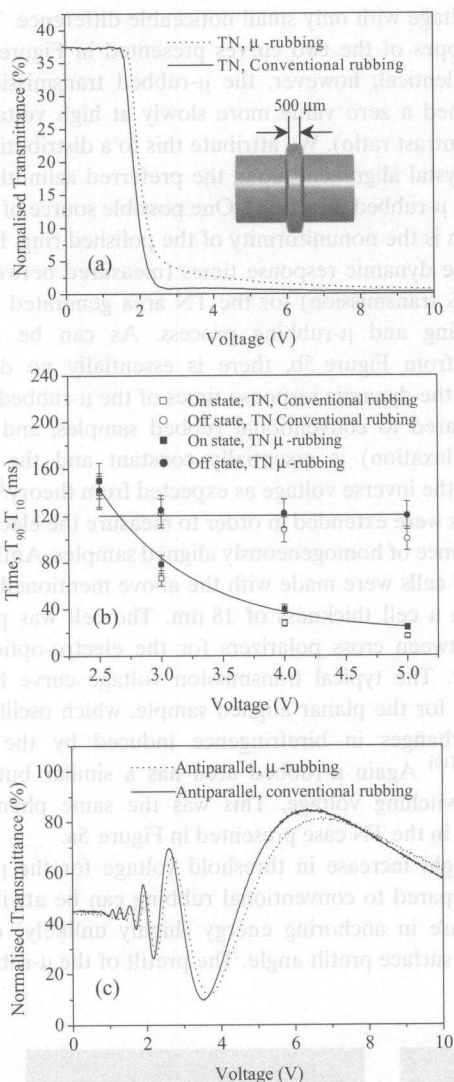


**Figure 5.** Comparison of the electro-optical characteristics of a) TN cell created by conventional rubbed polyimide layers and with  $\mu$ -rubbed orientation layers having a cell thickness of 18  $\mu\text{m}$ . b) Response and relaxation times for conventional TN cell and the TN area formed by the  $\mu$ -rubbing, under different fields at 1000 Hz. c) Electro-optic performance of anti-parallel cells (18  $\mu\text{m}$ ),  $\mu$ -rubbed and pre-rubbed, with a driving frequency of 1000 Hz.

the pre-rubbed polyimide were measured using a conoscopic technique.<sup>[20]</sup> Anti-parallel cells were made using the metallic ring with a cell spacing of 18  $\mu\text{m}$  and placed between cross polarizers with the optic axis parallel to the bottom polarizer direction. Figure 6 shows the conoscopic images of pre-rubbed and  $\mu$ -rubbed polyimide. For perfectly planar alignment of the liquid crystal at the surface with zero pre-tilt, the conoscopic pattern is characterized by a family of hyperboles that are symmetrically arranged into four quadrants. The shift of the pattern about the origin is a rough measure of the surface pre-tilt angle. It was found that the polyimide from the conventional rubbing method possessed a pre-tilt of  $2.6 \pm 0.5^\circ$ , which is consistent with specifications from the manufacturer. In the case of the  $\mu$ -rubbed polyimide, the conoscopic image

is nearly symmetrical, which indicates that the average pre-tilt is small. We measured the pre-tilt by carefully analyzing the position of the hyperbolic lines about the origin. The subtle difference in the symmetry of the conoscopic images can be observed in Figure 6. This observation of the decrease in pretilt of the  $\mu$ -rubbed polyimide is consistent with our observation that the Fredericks transition is slightly higher in the  $\mu$ -rubbing case, which is also in agreement with analytical models.<sup>[21]</sup> It is a subject of future study to more thoroughly investigate the anchoring energy and pre-tilt angle as a function of  $\mu$ -rubbing direction.

We have demonstrated that  $\mu$ -rubbing of polyimide substrates with a metallic sphere under well-defined conditions is an attractive method to generate patterned alignment layers. In accordance with previous studies by Yokoyama and co-workers, it was found that a planar alignment was generated by writing with a rigid (inorganic) tip in a rather soft polymeric substrate.<sup>[17]</sup> We disclosed that the pre-rubbing history of a polyimide substrate can be erased by a second rubbing procedure with a metallic sphere; this has also been observed using conventional rubbing techniques.<sup>[22,23]</sup> Apparently, this is a straightforward method that is used to obtain complete control over the planar alignment of liquid crystals. In our experiment, a single metallic sphere was used to write line patterns in the polyimide substrates and  $\mu$ -patterned alignment layers were created with typical pattern dimensions (width) on the same order of magnitude as the pixels in a liquid crystal display (20–100  $\mu\text{m}$ ). This latter feature potentially opens new routes to the large scale and high throughput production of patterned alignment layers for LCDs.

## Experimental

**Materials:** Indium tin oxide (ITO) coated glass substrate was purchased from Merck. The polyimide precursor, A11051 was used for the planar orientation layer (JSR electronics). Spin coating of the polyimide precursor was performed using a Karl Süss CT 62 spin coater (5 s at 1000 rpm, 40 s at 5000 rpm) on the ITO side of  $2.5 \times 2.5$  cm glass/ITO substrates. After spin coating, the substrates were pre-heated to 100 $^\circ$  C for 10 mins. The samples were then imidized at 180 $^\circ$  C for 90 mins in a vacuum oven. The thickness of the polyimide coating was 100 nm. Liquid crystal E7, a multi component cyanobiphenyl and terphenyl mixture ( $T_{NI}=60^\circ\text{C}$ ,  $\rho=1.06$  g cm $^{-3}$ ,  $\epsilon_{\parallel}=19$  and  $\epsilon_{\perp}=5.2$ , and  $\Delta n=0.225$ ) was used as obtained from Merck (Darmstadt, Germany)

**$\mu$ -Rubbing:** Uniaxial rubbing of polyimide substrates with a velvet cloth was performed at room temperature. The  $\mu$ -rubbing of polyimide substrates was carried out perpendicular to the rubbing direction with a mechanical device having a metallic sphere of 1 mm in diameter. Patterns were recorded by writing at a constant load and velocity at room temperature.

**Construction of Cell:** The electro-optical cells were constructed using ITO-coated glass with the polyimide substrates. A cell was constructed and secured with UV curable glue (Norland UV Sealant 91) having 18  $\mu\text{m}$  spacers. The cells are filled with liquid crystal material E7, by capillary action at 80  $^\circ\text{C}$ ,  $\sim 20^\circ\text{C}$  above the nematic–isotropic transition temperature of the LC.

**Characterization:** The patterns were investigated by scanning probe microscopy (Nanoscope IIIa, Digital Instruments, Santa Barbara, California) equipped with conventional  $\text{Si}_3\text{N}_4$  cantilevers and tips in

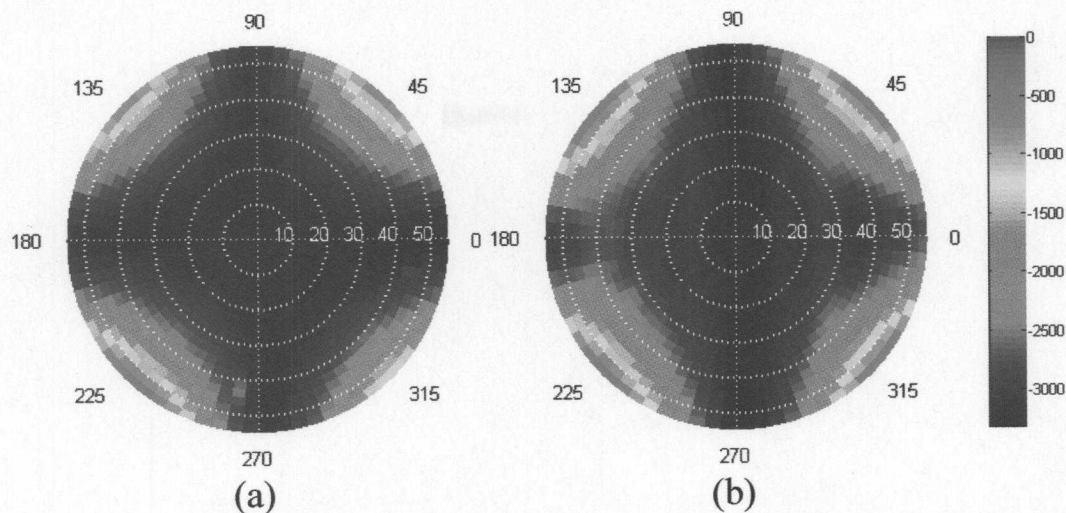


Figure 6. Shows the conoscopic images a) polyimide by conventional rubbing, anti-parallel cells (18  $\mu\text{m}$ ), b)  $\mu$ -rubbed, anti-parallel cells.

tapping mode. Optical micrographs were recorded with polarized light microscopy (Zeiss LM Axioplan) equipped with digital camera. The cell thickness was determined by UV-visible spectroscopy (Shimadzu UV-3102 PC).

**Electro-Optical Characterization:** The electro-optical characteristics were investigated using DMS 703 display measuring system (Autronic-Melchers GmbH). A square wave was used in order to drive the cells for the dynamic response measurements.

Received: November 26, 2003

Final version: April 8, 2004

Published online: September 8, 2004

- [16] B. Wen, M. P. Mahajan, C. Rosenblatt, *Appl. Phys. Lett.* **2000**, 76, 1240.  
 [17] J. H. Kim, M. Yoneya, H. Yokoyama, *Nature* **2002**, 420, 159.  
 [18] L. M. Blinov, V. G. Chigrinov, *Electro-optic effects in liquid crystal materials*, Springer-Verlag, New York **1996**, Ch. 4.  
 [19] P. Yeh, L. Gu, *Optics of liquid crystal displays*, John Wiley & Sons, New York **1999**, Ch. 5.  
 [20] B. L. V. Horn, H. H. Winter, *Appl. Opt.* **2001**, 40, 2089.  
 [21] J. Nehring, A. R. Kmetz, T. J. Scheffer, *J. Appl. Phys.* **1976**, 47, 850.  
 [22] J. Stohr, M. G. Samant, A. Cossy-Favre, J. Diaz, Y. Momoi, S. Odahara, T. Nagata, *Macromolecules* **1998**, 31, 1942.  
 [23] S. H. Paek, C. J. Durning, K. W. Lee, A. Lien, *J. Appl. Phys.* **1998**, 83, 1270.

- [1] J. M. Geary, J. W. Goodby, A. R. Kmetz, J. S. Patel, *J. Appl. Phys.* **1987**, 62, 10.  
 [2] S. W. Depp, W. E. Howard, *Sci. Am.* **1993**, 266, 40.  
 [3] S. Musa, *Sci. Am.* **1997**, 277, 87.  
 [4] M. Schadt, W. J. Helfrich, *Appl. Phys. Lett.* **1971**, 18, 127.  
 [5] N. A. J. M. van Aerler, *J. Soc. Inf. Display* **1994**, 2, 41.  
 [6] A. Fukuro, K. Sawahata, T. Sato, H. Endo, *SID International Symposium*, **2000**, XXXI, 434.  
 [7] M. Neill, S. M. Kelly, *J. Phys. D* **2000**, 33, R67.  
 [8] M. Schadt, H. Seiberle, A. Schuster, *Nature* **1996**, 381, 212.  
 [9] A. T. Ionescu, R. Barberi, M. Giocondo, M. Lovace, A. L. A. Ionescu, *Phys. Rev. E* **1998**, 58, 1967.  
 [10] R. Yamaguchi, Y. Goto, S. Sato, *Jpn. J. Appl. Phys. Part 2* **2002**, 41, L889.  
 [11] P. Chaudhari, J. Lacey, J. Doyle, E. Galligan, S.-C. A. Lien, A. Callegari, G. Hougham, N. D. Lang, P. S. Andry, R. John, K.-H. Yang, M. A. Lu, C. Cai, J. Speidell, S. Purushothaman, J. Ritsko, M. Samant, J. Stöhr, Y. Nakagawa, Y. Katoh, Y. Saitoh, K. Sakai, H. Satoh, S. Odahara, H. Nakano, J. Nakagaki, Y. Shiota *Nature* **2001**, 411, 56.  
 [12] A. Kumar, N. L. Abbott, H. A. Biebuyck, G. M. Whitesides, *Acc. Chem. Res.* **1995**, 28, 219.  
 [13] J. L. Wilbur, A. Kumar, E. Kim, G. M. Whitesides, *Adv. Mater.* **1994**, 6, 600.  
 [14] H. T. A. Wilderbeek, F. J. A. der Meer, K. Feldman, D. J. Broer, C. W. M. Bastiaansen, *Adv. Mater.* **2002**, 14, 655.  
 [15] G. P. Sinha, C. Rosenblatt, L. V. Mirantsev, *Phys. Rev. E* **2002**, 65, 041718.

## Visualizing Ion Currents in Conjugated Polymers\*\*

By Xuezheng Wang, Benjamin Shapiro, and Elisabeth Smela\*

In numerous technologically important materials, electrochemical reactions are accompanied by the mass transport of charged particles. For example, ion ingress and egress during

[\*] Dr. E. Smela, X. Wang  
 Department of Mechanical Engineering, University of Maryland  
 College Park, MD 20742 (USA)  
 E-mail: smela@eng.umd.edu

Dr. B. Shapiro  
 Department of Aerospace Engineering, University of Maryland  
 College Park, MD 20742 (USA)

[\*\*] This material is based upon work supported in part by the U. S. Army Research Laboratory and the U. S. Army Research Office under contract number DAAD190310085. We also acknowledge the U. S. Army Research Laboratory for use of equipment while completing this research and funding through DuPont's Educational Aid Program (Young Professor Grant).